Influence of Bending Stresses on Fatigue Crack Propagation Life in Butt Joint Welds

Small joint distortions resulting from welding can induce significant bending stresses which should be considered in calculating fatigue crack propagation life

BY J. D. BURK AND F. V. LAWRENCE

ABSTRACT. The fatigue crack propagation life of A-36 steel double-V groove welds in butt joints was determined for the conditions of zero-to-tension axial loads. Good agreement between the measured and calculated fatigue crack propagation lives could be obtained only when the bending stresses resulting from joint straightening under load were considered in the analysis. The magnitude of these bending stresses was found to be surprisingly large, and expressions are presented which predict this effect.

Previous Work

A large portion of the fatigue life of welds is spent in fatigue crack propagation. The fatigue crack propagation fraction of life (N_{pc}) can be considered to be a lower bound of total fatigue life and can be estimated through the use of the relationship between range in crack tip stress intensity factor (ΔK) and crack growth rate per cycle (dc/dN) (Ref. 1):

$$\Delta K = \Delta S\sqrt{\pi c}\ (\gamma) \qquad (1)$$

$$dc/dN = C(\Delta K)^n \qquad (2)$$

$$N_{pc} = \int_{c_o}^{c_f} (1/C(\Delta K)^n)\ da \qquad (3)$$

where: c_o = initial crack length; c_f = final crack length; C,n = material constants; ΔK = stress intensity factor range; ΔS = stress range; γ = function of crack length and geometry.

Several difficulties arise in applying Eqs. 1-3 to welds; welds such as groove and fillet welds have complex geometries and loading conditions. The correct value of initial flaw size (c_o) is unclear for defect-free welds, and the choice of c_o can greatly influence the value of N_{pc} obtained. In addition, this analysis is, at present, most conveniently applied to constant stress amplitude, positive stress ratio circumstances ($R > 0$).

With these limitations in mind, several investigators have been studying the influence in weld geometry, material properties, and loading conditions on N_{pc}. Maddox (Ref. 2) has considered the influence of crack shape (ellipticity), plate thickness (finite width corrections), and weld reinforcement shape, for fillet welds through a series of corrections to Eq. 1. Lawrence (Ref. 3) has used an elastic superposition method to study the influence of weld geometry and material properties on N_{pc} in butt welds.

In the current study, the elastic superposition method has been used to investigate the influence of combined bending and axial loads.

Calculation of N_{pc} under Combined Axial and Bending Stresses

To calculate N_{pc} (Eq. 3), the range in stress intensity factor (ΔK) (Eq. 1) must be known as a function of crack length (c) for a given weld geometry. The elastic superposition method (Ref. 3) enables one to determine (ΔK) through a single finite element analysis of the crack-free weld geometry. By determining the stresses in the crack-free weld, and particularly the stresses perpendicular to the eventual crack path, one can determine ΔK

List of Symbols

α, θ, ϕ	Distortion, flank, and edge preparation angles
ϵ, ϵ_1, ϵ_2, ϵ_1', ϵ_2'	Bending strain, initial strains 1 and 2, and instantaneous strains 1 and 2
ΔK, ΔK_A, ΔK_B	Range in stress-intensity for applied general, axial, and bending stresses
σ, S	Stress along crack interface and remote applied stress
ΔS, ΔS_A, ΔS_B	Applied general, axial, and bending stress range
S_{Bp}, S_{Bf}	Bending stress from pinned or fixed ended conditions
dc/dN	Crack growth per cycle
C,n	Crack propagation material constants
R	Stress ratio
E	Young's modulus
L	Length of test piece
M	Induced moment in weld at L/2
M_o	Induced moment in weld at L/2 neglecting joint straightening
h,w,t	Weld bead height and width, plate thickness
N_p, N_T	Fatigue crack propagation and total life
N_{pc}, $N_{pmeas.}$	Calculated and measured fatigue crack propagation life
N_I	Measured fatigue life to initiate a detectable 0.01 in. fatigue crack
x,y	Local coordinates at the weld toe
c, c_o, c_f	Crack length and initial and final crack length
$a_1 \ldots a_3$, $b_1 \ldots b_3$	Axial and bending constants used in stress polynomial
γ	Generalized correction factor (function of crack length and specimen geometry)

J. D. BURK is Graduate Research Assistant, Department of Metallurgy and Mining Engineering, and F. V. LAWRENCE is Associate Professor of Civil and Metallurgical Engineering, University of Illinois at Urbana-Champaign, Ill.

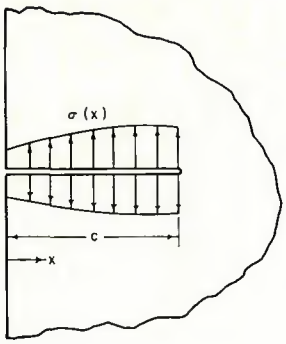

$$K = \sqrt{\pi c}\left\{1.1\,\sigma - \int f\left(\frac{x}{c}\right)\cdot\frac{d\sigma}{dx}\,dx\right\}$$

$$f\left(\frac{x}{c}\right) = 0.8\left(\frac{x}{c}\right) + 0.04\left(\frac{x}{c}\right)^2 + 3.62 \times 10^{-6} \times e^{11.18\left(\frac{x}{c}\right)}$$

Fig. 1—Stress intensity factor for an edge crack loaded with an arbitrary system of internal stresses (Ref. 4)

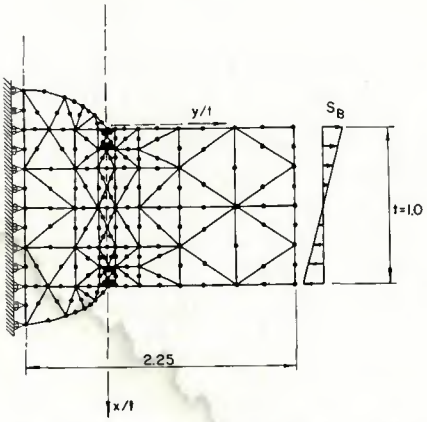

Fig. 2—Finite element mesh for pure bending

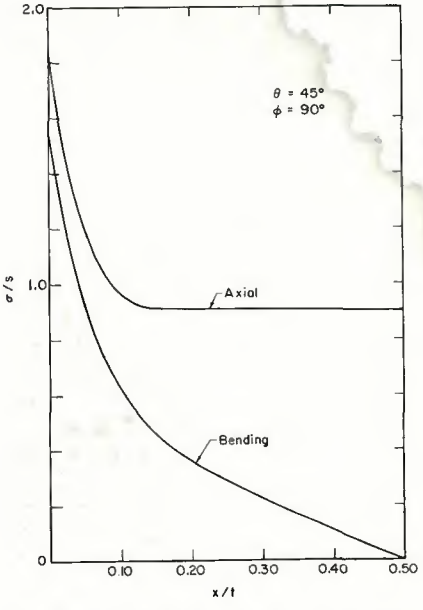

Fig. 3—Axial and bending stress profiles inward from the weld toe

using elastic superposition and Emery's solution (Ref. 4) for an edge crack pulled open by an arbitrary system of stresses (σ), see Fig. 1:

Table 1—Coefficients for Bending (Eq. 5)

ϕ, deg	θ, deg	b_1	b_2	b_3	b_4	b_5
30	0	1.0	−2.0	0	0	0
	10	1.018	−4.80	21.32	−57.30	51.55
	20	1.169	−7.94	43.78	−118.96	107.91
	30	1.211	−9.40	54.90	−149.85	136.35
	45, 60	1.265	−10.68	64.68	−177.12	161.34
45	0	1.0	−2.0	0	0	0
	10	1.088	−6.14	30.09	−80.19	71.94
	20	1.221	−9.07	50.41	−134.37	120.57
	30	1.311	−11.15	64.96	−173.52	155.93
	45, 60	1.325	−11.98	71.53	−192.02	173.07
60	0	1.0	−2.0	0	0	0
	10	1.075	−6.01	28.62	−75.51	67.65
	20	1.254	−9.84	54.41	−143.58	128.62
	30	1.359	−12.46	72.79	−193.13	173.63
	45, 60	1.423	−14.25	85.70	−228.24	205.64
90, 120	0	1.0	−2.0	0	0	0
	10	1.056	−6.07	28.68	−74.84	66.81
	20	1.278	−10.93	61.57	−162.15	145.48
	30	1.434	−14.25	83.80	−220.78	198.11
	45, 60	1.54	−17.09	103.47	−273.51	245.95

Table 2—Coefficients for Axial Loads (Eq. 6)

ϕ, deg	θ, deg	a_1	a_2	a_3	a_4	a_5
30	0	1.0	0	0	0	0
	10	1.098	−2.41	16.06	−40.65	35.78
	20	1.205	−5.17	35.91	−89.92	76.39
	30	1.241	−6.16	41.78	−107.64	92.74
	45, 60	1.280	−7.40	51.77	−130.40	112.60
45	0	1.0	0	0	0	0
	10	1.18	−4.12	26.51	−65.86	55.78
	20	1.27	−5.84	37.53	−93.23	78.94
	30	1.34	−7.93	51.60	−129.04	109.72
	45, 60	1.38	−9.28	61.65	−156.32	134.23
60	0	1.0	0	0	0	0
	10	1.261	−5.41	33.45	−81.74	68.66
	20	1.419	−8.73	53.98	−131.82	110.66
	30	1.537	−11.34	70.55	−174.84	145.38
	45, 60	1.618	−13.27	82.98	−203.74	171.54
90	0	1.0	0	0	0	0
	10	1.364	−7.09	42.84	−104.20	87.52
	20	1.563	−10.97	66.25	−161.05	135.20
	30	1.717	−14.03	84.72	−205.97	172.92
	45, 60	1.831	−16.57	100.54	−244.88	205.74
120	0	1.0	0	0	0	0
	10	1.374	−7.56	49.33	−129.94	116.71
	20	1.623	−12.69	84.64	−225.73	203.72
	30	1.815	−16.21	104.71	−274.77	246.42
	45, 60	2.008	−21.13	142.00	−380.07	343.78

$$\Delta K = \sqrt{\pi c}\,[1.1\sigma - \int_0 f(x/c)\,(d\sigma/dx)\,dx] \qquad (4)$$

$$f(x/c) = 0.8(x/c) + 0.04(x/c)^2 + 0.352 \times 10^{-3} \exp 11.18(x/c)$$

where: c = crack length; x = coordinate along crack surface; σ = crack surface stresses.

As an illustration of this method, consider a weld in a butt joint subjected to pure bending. The finite element network for obtaining the stresses along the eventual crack path (σ) in Eq. 4 is shown in Fig. 2. The stresses so obtained are plotted in Fig. 3. To facilitate calculation of ΔK (Eq. 4), a fourth order polynomial is fitted to the crack path stresses, substituted into Eq. 4, and integrated, yielding (for $C_f < 0.2t$) (Ref. 5):

$$\Delta K_B = \Delta S_B \sqrt{\pi c}\,[1.1\,b_1 + 0.6635\,b_2(c/t) + 0.5255\,b_3(c/t)^2 + 0.4566\,b_4(c/t)^3 + 0.4153\,b_5(c/t)^4] \qquad (5)$$

where: ΔK_B = stress intensity factor for pure bending; ΔS_B = remote extreme fiber stress due to bending component of load; $b_1 \ldots b_5$ = coefficients for bending; t = plate thickness; c = crack length.

The constants b_1, b_2, b_3, b_4, b_5, for the case of bending vary with weld geometry and are listed in Table 1. A similar equation was derived for the case of

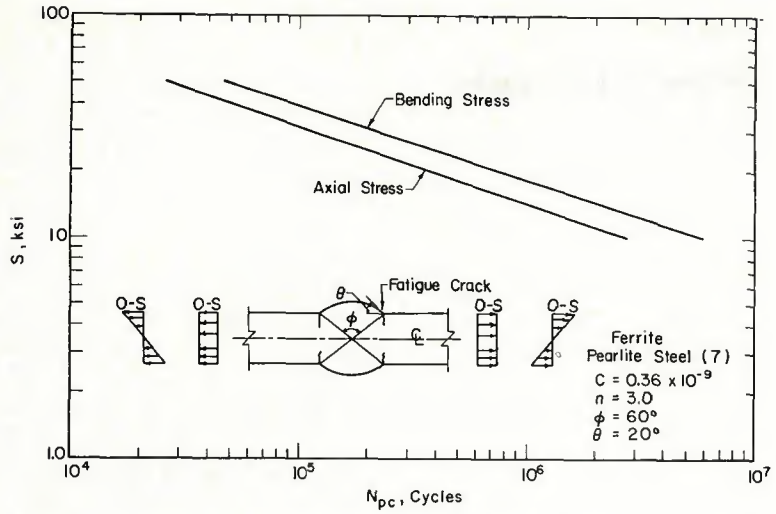

Fig. 4—Difference in N_{pc} resulting from pure bending and axial remote stresses

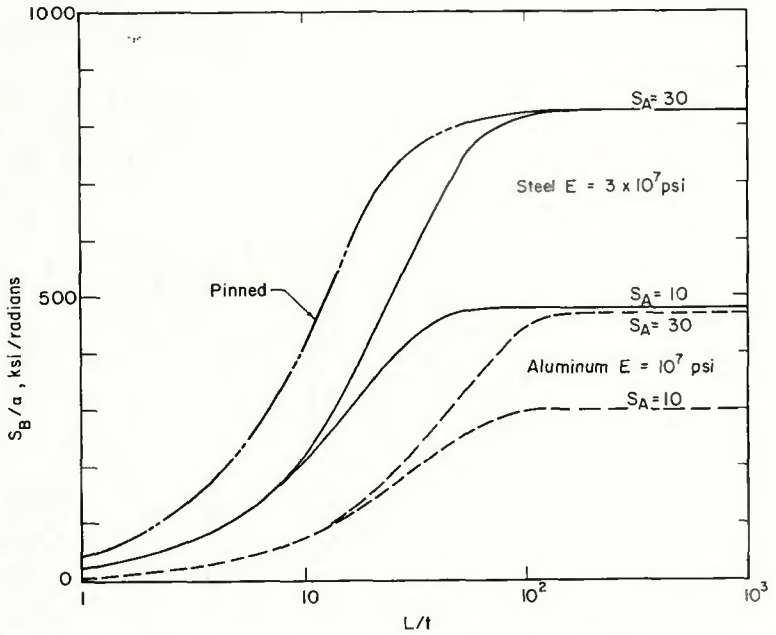

Fig. 6—S_B/α versus L/t. Aluminum: dashed lines; steel: solid lines. All results for fixed ends, except as noted

pure axial stresses:

$$\Delta K_A = \Delta S_A \sqrt{\pi c}\,[1.1\ a_1 + 0.6635\ a_2(c/t) + 0.5255\ a_3(c/t)^2 + 0.4566\ a_4(c/t)^3 + 0.4153\ a_5(c/t)^4] \quad (6)$$

where: ΔK_A = stress intensity factor due to axial load; ΔS_A = remote axial stress component of load; $a_1 \ldots a_5$ = coefficients for axial conditions; t = plate thickness; c = crack length.

The constants a_1 through a_5 vary with weld geometry and are listed in Table 2.

The stress intensity factor for combined axial and bending loads can be obtained by superposing the ΔK found for the axial and bending components:

$$\Delta K = \Delta K_A + \Delta K_B \quad (7)$$

The above analysis does not consider the effects of finite plate width since only a small fraction of N_{pc} is affected by this inaccuracy. Also the effects of crack ellipticity are not considered since it has been our practice to begin the N_{pc} calculation at initial crack lengths (c_o) sufficiently large to avoid both the low ΔK region and the effects of ellipticity. Our customary assumption for c_o has been a crack depth of 0.01 in. (0.25 mm) which dimension is also the smallest crack length we can nondestructively detect in laboratory tests.

Bending Induced by Heat Distortions

Bending stresses are less severe than axial stresses of the same magnitude. In ferritic-pearlitic steels, the N_{pc} for pure bending is three times that of

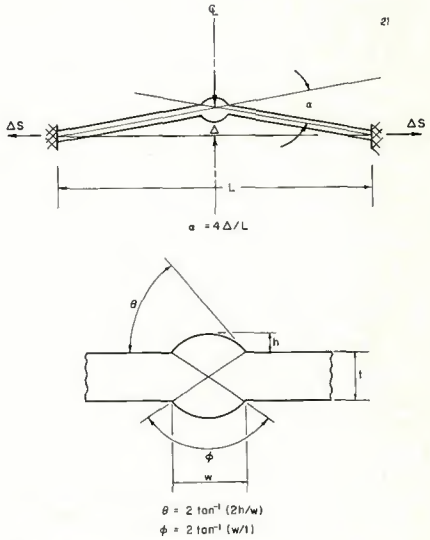

Fig. 5—Specimen geometry

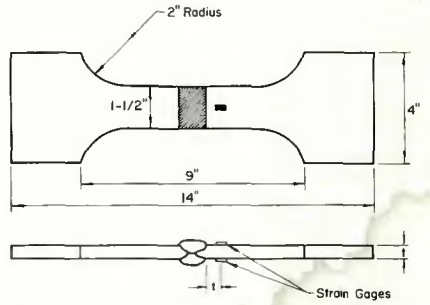

Fig. 7—A-36 steel butt joint fatigue test pieces

remotely applied axial stresses (see Fig. 4). Even though bending stresses produce a lesser effect than axial stresses, bending stresses cannot be neglected in situations involving combined bending and axial loads.

One commonly overlooked situation which involves both axial and bending loads is the nominal zero to tension axial load. In this case, the bending is induced by the straightening under load of the small angular joint distortions produced by welding. In double-V groove welds, these angular distortions may be imperceptably small; whereas, in single-V groove welds and fillet welds, these distortions may be evident to the eye.

The bending stresses induced by partial straightening under load (see Fig. 5) can be calculated using the expressions below (Ref. 6). For pin ended conditions:

$$M/M_o = \tanh \beta/\beta, \quad (\beta = (L/t)\sqrt{3S_A/E}) \quad (8)$$

$$S_{Bp}/\alpha = (3/2)S_A(L/t)\tanh \beta/\beta \quad (9)$$

With ends fixed against rotation:

$$M/M_o = [\tanh(\beta/2)]/(\beta/2) \quad (\beta = \text{same as above}) \quad (10)$$

$$S_{Bf}/\alpha = (3/4)\,S_A\,(L/t)[\tanh(\beta/2)/(\beta/2)] \quad (11)$$

Table 3—Specimen Geometry and Measured Strains

Specimen	Thickness, in.	Distortion angle α, radians	Flank angle θ, deg	Edge prep. angle ϕ, deg	Strain 1, $\epsilon_1 \times 10^6$, μ in./in.	Strain 2 $\epsilon_2 \times 10^6$ μ in./in.	Bending strain, $\epsilon_B \times 10^6$ μ in./in.
18	3/8	0.0100	66	90	1370	920	225
19	3/8	0.0054	75	88	1030	1030	0
20	3/8	0.0110	74	90	1485	830	325
21	3/8	0.0134	70	90	1675	915	380
23	3/8	0.0094	79	86	1285	1140	70
24	3/8	0.0124	75	88	1110	705	200
25	3/8	0.0120	74	90	905	510	150
26	3/8	0.0134	70	86	880	585	150
27	3/8	0.0044	72	88	970	685	90
28	3/8	0.0046	70	90	960	665	150
29	3/8	0.0044	68	90	1080	600	240
61	5/8	0.0160	35	100	1235	1110	60
62	5/8	0.0014	50	94	1225	1145	40
65	5/8	0.0016	52	97	1315	1110	100
69	5/8	0.0046	47	99	1190	1140	25
71	5/8	0.0058	47	100	1170	980	95
74	5/8	0.0036	43	98	1120	1100	10
64	5/8	0.0080	52	96	835	790	20
66	5/8	0.0016	48	95	1000	700	150
68	5/8	—	45	100	980	740	120

where: M = induced moment at L/2; M_o = induced moment at L/2 without joint straightening; L = test piece length; t = plate thickness; S_A = applied axial stress; E = Young's modulus; S_{Bp} = induced bending stress at L/2 for pin ended conditions; S_{Bf} = induced bending stress at L/2 for fixed ended conditions; α = joint distortion (radians).

As an example, consider a steel weld having a joint distortion (α) of 0.1 degree (0.0017 radians). If S_A = 30 ksi (207 MPa), L = 100 in. (2540 mm), t = 1 in. (25.4 mm), then S_B is approximately ± 1.4 ksi (10 MPa) for both the fixed ended and pinned cases. For (L/t) larger than 100, S_B is independent of both the end conditions, and (L/t) depends solely upon $\sqrt{S_A E}$, and attains its largest value (see Fig. 6):

$$S_{Bp}/\alpha = S_{Bf}/\alpha \cong \sqrt{3/2}\sqrt{S_A E}; \quad (L/t) > 100 \qquad (12)$$

For small (L/t) S_{Bp} is twice S_{Bf} for a given α.

Table 4—Fatigue Test Results for A36 Butt Joint Specimens

Specimen	Stress range, ΔS_A, ksi (MPa)	Bending stress, ΔS_B, ksi (MPa)	Life, N_T, cycles	Crack propagation life, $N_{Pmeas.}$, cycles
18	33 (227.5)	7.1 (48.9)	181,000	65,000
19	33 (227.5)	0 (0)	195,000	80,000
20	33 (227.5)	10.8 (74.5)	226,000	71,000
21	33 (227.5)	12.7 (87.5)	297,000	99,000
23	33 (227.5)	2.3 (15.8)	299,000	129,000
24	24 (165.5)	6.7 (46.2)	887,000	437,000[b]
25	19 (131.0)	5.0 (34.5)	9,680,000[a]	—
26	21 (144.8)	5.0 (34.5)	9,130,000[a]	—
27	24 (165.5)	3.0 (20.7)	1,960,000	230,000
28	24 (165.5)	5.0 (34.5)	974,000	264,000
29	24 (165.5)	8.0 (55.2)	1,160,000	160,000
61	33 (227.5)	2.0 (13.8)	212,300	104,000
62	33 (227.5)	1.3 (9.0)	153,000	55,000
65	33 (227.5)	3.3 (22.7)	213,000	97,000
69	33 (227.5)	0.8 (5.5)	190,000	71,000
71	33 (227.5)	3.2 (22.1)	182,000	92,000
74	33 (227.5)	0.3 (2.1)	258,000	78,000
64	24 (165.5)	0.7 (4.8)	586,800	224,000
66	24 (165.5)	5.0 (34.5)	438,000	138,000
68	24 (165.5)	4.0 (27.6)	694,000	255,000

(a) Failure did not occur
(b) Crack propagation occurred at less than 437,000 cycles

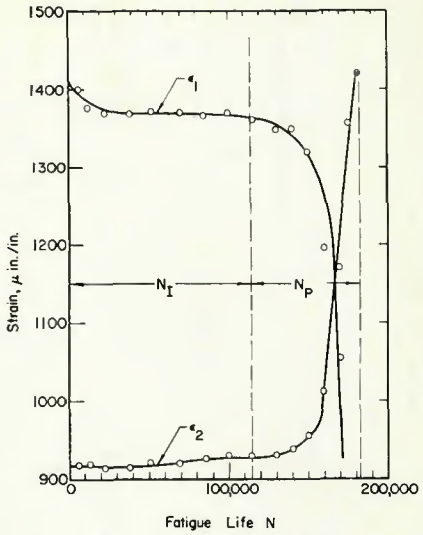

Fig. 8—Variation of peak strains with life

Fatigue Tests on Double-V Groove Welds

Butt joints with full penetration double-V groove welds were prepared using 3/8 in. (9.5 mm) and 5/8 in. (15.9 mm) thickness ASTM A-36 steel plate. The welds were made in the flat position with one pass per side using GMAW equipment, Ar-2% O_2 shielding gas and an E70 grade electrode. Test pieces similar to those shown in Fig. 7 were machined. The angles defining the weld geometry (θ ϕ) and joint distortion (α) were measured and are listed in Table 3. Strain gages (micro measurements EA series) were mounted on each side of the plate near the weld toe. The gages were located a distance equal to the plate thickness away from the weld to avoid the stress concentration in the latter.

The test pieces were fatigued in a closed-loop, hydraulic mechanical testing system (M.T.S.) at a frequency of 20 Hz, under ambient laboratory conditions. Periodic measurements were made of the peak (dynamic) strain on each side of the weld using peak reading meters. A typical peak strain record is shown in Fig. 8.

The strain readings provide two types of important information. The bending component of stress can be calculated from the initial differences in peak strain between the two sides: (ϵ_1', ϵ_2').

$$\pm \epsilon_B = (1/2)(\epsilon_{1_0}' - \epsilon_{2_0}') \qquad (13)$$

Secondly, it will be noticed in Fig. 8 that the peak strains remain relatively constant but begin to change simultaneously at a certain point in the fatigue test. Usually the higher peak strain (ϵ_1) will decrease while lower peak strain (on the opposite side of the test piece) (ϵ_2) will increase. This event is caused by the presence of a small toe crack on the higher peak

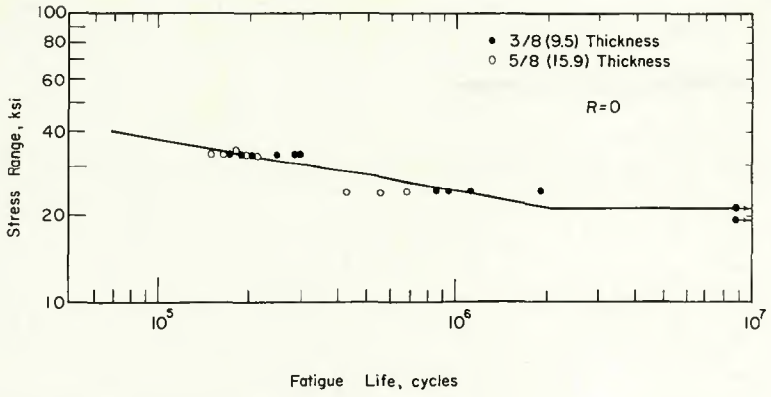

Fig. 9—S-N curve for A-36 butt joints

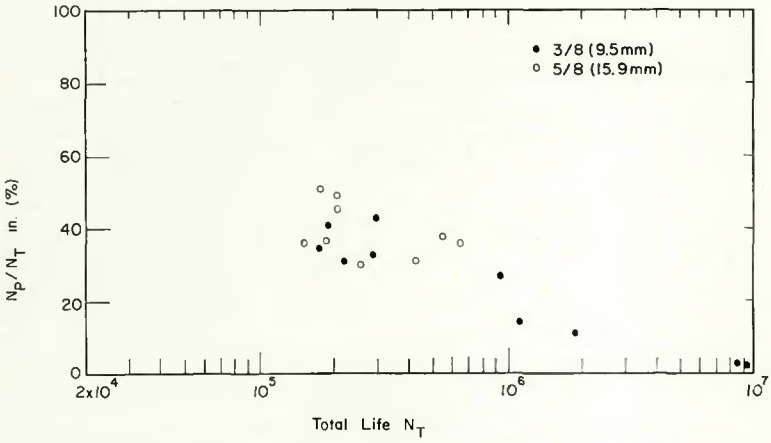

Fig. 10—Percentage of fatigue life spent in crack propagation as a function of total life

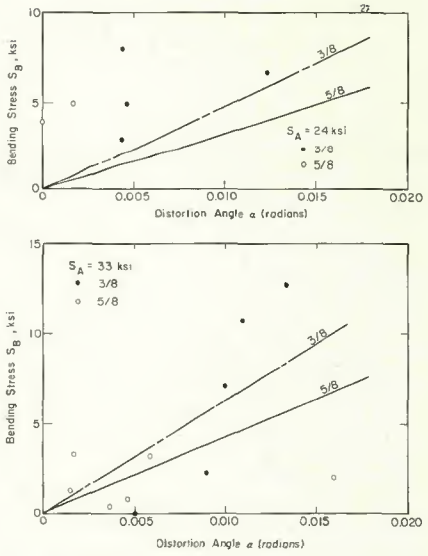

Fig. 11—Calculated and measured bending stresses

strain side. Auxiliary tests and destructive examination of the test pieces showed that the point at which these changes could be observed corresponded to the presence of a 0.01 in. (0.25 mm) depth fatigue crack at the most highly stressed weld toe. By monitoring changes in the quantity

$$\Delta \epsilon = |\epsilon_1 - \epsilon_2| - \epsilon_B, \qquad (14)$$

the point at which a 0.01 in. depth fatigue crack was present could be identified, and the measured total fatigue life could be separated into a crack initiation and crack propagation portion consistent with our definition given earlier.

The results of these experiments are summarized in Tables 3 and 4 and Figs. 9 and 10. The 3/8 in. (9.5 mm) welds gave slightly longer total lives at the lower stress levels due to a greater number of cycles spent in creating a 0.01 in. fatigue crack. This effect is possibly due to residual stress differences. As shown in Fig. 10, the fraction of fatigue life spent in crack propagation decreases as total life increases.

Bending Stresses Induced by Joint Distortions

A comparison of the measured bending stresses and those calculated using Eq. 11 is shown in Fig. 11. The agreement between the calculated and measured values is considered reasonable particularly when it is realized that the end conditions of the test pieces may not be rigidly fixed against rotation as is assumed in Eq. 11. Slight end rotations will allow higher bending stresses to be generated at midlength, but in no case should the measured stresses exceed twice the calculated values since this would correspond to pin ended conditions.

Equation 11 correctly predicts that the induced bending stresses will increase linearly with joint distortion (α) and that the bending stress will be greater in the thinner test pieces for a given joint distortion at small L/t.

Figure 6 shows the influence of test piece length to thickness ratio (L/t), applied axial stress (S_A), and Young's Modulus (E) upon the ratio of the induced bending stress to joint distor-

Table 5—Comparison of Calculated and Measured Crack Propagation Lives

Specimen	Total life, N_T	Crack propagation life, $N_{Pmeas.}$	Calculated N_{Pc} with $S_B = 0$	Calculated N_{Pc} using bending stresses	Life to initiate 0.01 in. crack, N_i
18	181,000	65,000	120,000	96,000	116,000
19	195,000	80,000	120,000	120,000	115,000
20	226,000	71,000	120,000	63,000	155,000
21	297,000	99,000	120,000	51,000	198,000
23	299,000	129,000	120,000	103,000	170,000
24	887,000	437,000[a]	345,000	206,000	450,000
25	9,680,000	—	—	—	9,680,000
26	9,130,000	—	—	—	9,130,000
27	1,960,000	230,000	345,000	255,000	1,730,000
28	974,000	264,000	345,000	227,000	710,000
29	1,160,000	160,000	345,000	170,000	1,000,000
61	212,300	104,000	105,000	89,000	108,300
62	153,000	55,000	105,000	93,000	98,000
65	213,000	97,000	105,000	83,000	116,000
69	190,000	71,000	105,000	98,000	119,500
71	182,000	92,000	105,000	83,000	90,000
74	258,000	78,000	105,000	104,000	180,000
64	586,800	224,000	305,000	276,000	362,800
66	438,000	138,000	305,000	171,000	300,000
68	694,000	255,000	305,000	206,000	439,000

(a) Crack propagation occurred at less than 437,000 cycles.

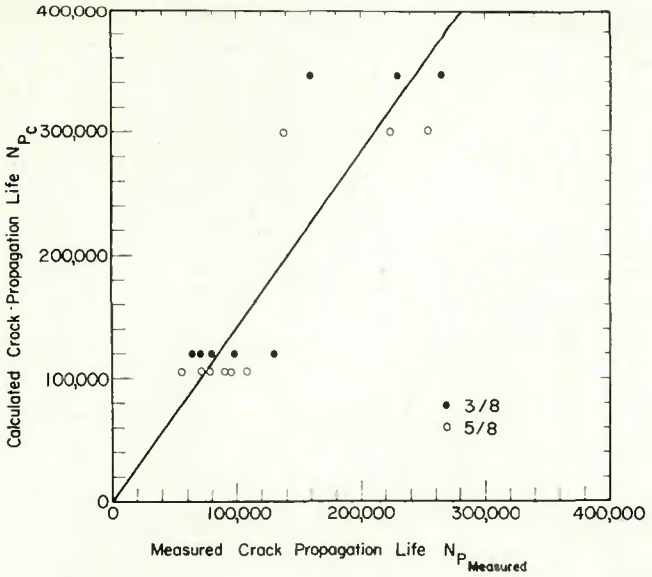

Fig. 12—Calculated and measured N_p considering only axial stresses

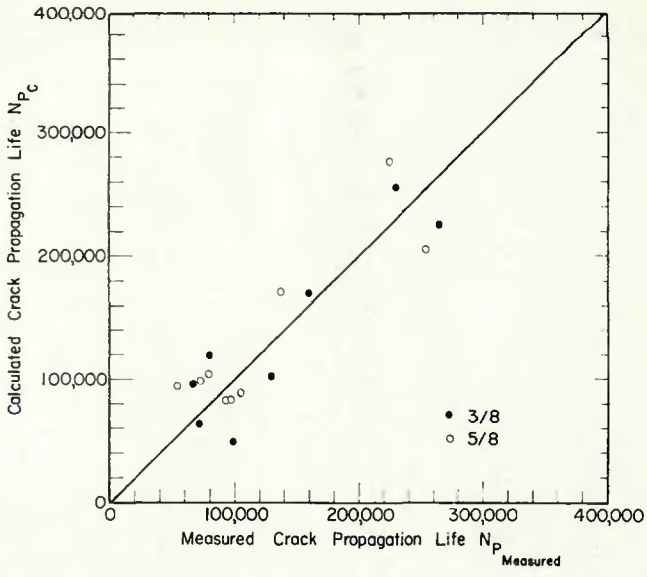

Fig. 13—Calculated and measured N_p considering both axial and induced bending stresses

tion (S_B/α). The induced bending stresses would not be as large in aluminum welds under similar conditions.

Influence of Joint Distortions on N_{pc}

As seen in Table 4 and Fig. 11 the measured bending stresses (S_B) resulting from the joint distortion (α) range from very small values ($\sim$0) to values as large as 12.7 ksi (87.6 MPa). If one calculates N_{pc} using values of $C = 10^{-10}$ in./cycle and $n = 3.3$ reported by Barsom (Ref. 7) for ASTM A-36 steel and ignores the induced bending, the comparison between calculated and measured crack propagation life is reasonable as seen in Fig. 12 and Table 5, but when the induced bending stresses are considered, the agreement is very good (see Fig. 13). This observation leads to the conclusion that the bending stresses induced by joint distortions as well as the effects of weld reinforcement shape should be considered in fatigue crack propagation life calculations.

Whether one considers the number of cycles required to produce a 0.01 in. crack to be crack initiation or crack propagation at low ΔK values, it is clear from Fig. 10 that a substantial portion of fatigue life is devoted to this period; moreover, at low stress levels and long lives, this period becomes increasingly dominant (Ref. 8).

Conclusions

1. The fatigue crack propagation life calculation for combined axial and bending stresses may be obtained by elastic superposition of the stress intensity factors of the axial and bending components of stress.
2. Small joint distortions resulting from welding can induce significant bending stresses which should be taken into account in the calculation of the fatigue crack propagation life.
3. The induced bending stresses depend upon Young's Modulus, the size of the joint distortion, the end conditions, the level of applied stress and the ratio of test piece length to thickness. Expressions derived to predict this effect agree with measured bending stresses.
4. The fatigue crack propagation life which was defined as the fraction of life in which a 0.01 in. (0.25 mm) fatigue crack propagates to failure was one half or less of the total fatigue life.

Acknowledgments

The results of this study are based upon the Master's Thesis of Mr. J. D. Burk, the funds for which were provided by the Fracture Control Program at the University of Illinois at Champaign-Urbana. The Fracture Control Program is supported by a consortium of mid-west ground vehicle industries.

The authors wish to thank the John Deere Company for providing the welded test pieces used in the study. The authors wish to acknowledge the help of Professor A. R. Robinson of the Department of Civil Engineering in developing the expressions for induced bending moment. The authors also benefited from numerous helpful discussions with Professor W. H. Munse, also of the Civil Engineering Department.

References

1. Paris, P. C. and Erdogan, F., "A Critical Analysis of Crack Propagation Laws," *J. Basic Eng.* ASME Trans. Series D, Vol. 85, p. 528, 1963.
2. Maddox, S. J., "Assessing the Significance of Flaws in Welds Subject to Fatigue," *Welding Journal*, 53(9), Res. Suppl., 1974, p 401-s.
3. Lawrence, F. V., "Estimation of Fatigue-Crack Propagation Life in Butt Welds," *Welding Journal*, 52(5), Res. Suppl., 1973, p 212-s.
4. Emery, A. F., "Stress-Intensity Factors for Thermal Stresses in Thick Hollow Cylinders," *J. Basic Eng.* ASME Trans. Series D, Vol. 88, p. 45, 1966.
5. Burk, J. D., "Prediction of the Fatigue Crack Propagation Lives of Butt Weldments Subjected to Axial and Bending Stresses," M.S. Thesis, University of Illinois, Urbana, 1974.
6. Robinson, A. R., Private Communication, Professor, Department of Civil Engineering, University of Illinois, Urbana, 1976.
7. Barsom, J. M., "Fatigue-Crack Propagation in Steels of Various Yield Strengths," *J. Eng. Ind.*, ASME Series B, Vol. 93, p. 1190, 1971.
8. Mattos, R. J., "Estimation of the Fatigue Crack Initiation Life in Welds Using Low Cycle Fatigue Concepts," Ph.D. Thesis, University of Illinois, Urbana, 1975.